Highly Transparent Multifunctional Bilayer Coatings on Polymers Using Low-Temperature Atmospheric Plasma Deposition

Linying Cui,[†] Krystelle Lionti,[‡] Alpana Ranade,[§] Kjersta Larson-Smith,[§] Geraud Jean-michel Dubois,[†,‡,*] and Reinhold H. Dauskardt[†,*]

[†]Department of Materials Science and Engineering, Stanford University, Stanford, California 94305, United States, [‡]IBM Almaden Research Center, San Jose, California 95120, United States, and [§]Chemical Technology Division, Boeing Research & Technology, Seal Beach, California 90740, United States

ABSTRACT

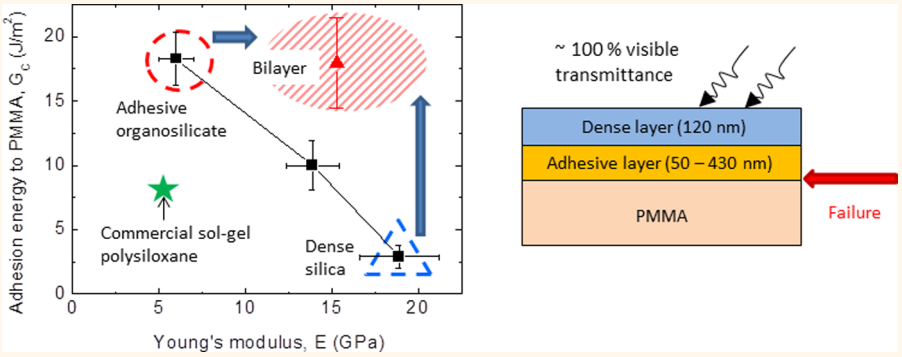

We report on the synthesis of hard, adhesive, and highly transparent bilayer organosilicate thin films on large poly(methyl methacrylate) substrates by atmospheric plasma, in ambient air, at room temperature, in a one-step process, using a single precursor. The method overcomes the challenge of fabricating coatings with high mechanical and interfacial properties in a one-step process. The bottom layer is a carbon-bridged hybrid silica with excellent adhesion with the poly(methyl methacrylate) substrate, and the top layer is a dense silica with high Young's modulus, hardness, and scratch resistance. The bilayer structure exhibited ~100% transmittance in the visible wavelength range, twice the adhesion energy and three times the Young's modulus of commercial polysiloxane sol–gel coatings.

KEYWORDS: bilayer · transparent · multifunctional coatings · atmospheric plasma deposition · low temperature · one-step process

Highly adhesive and transparent protective coating deposition on large polymer substrates is an important technological challenge for flexible electronics, photovoltaic panels, and polymer windows. Low adhesion between the protective layers and the polymer substrates poses significant reliability issues for devices.[1−3] From a synthetic and processing point of view, it is extremely challenging to fabricate, in a one-step deposition process, coatings with high mechanical and interfacial properties. Indeed, the thin film chemistry and the deposition conditions required to optimize these two properties significantly differ from each other. Typically, the interfacial adhesion of inorganic oxides or nitrides with polymers is low due to the lack of covalent bonds.[4,5] For example, the interfacial adhesion between sol–gel silica and polycarbonate can be as low as 2 J/m^2,[6] lower than the ~5 J/m^2 benchmark minimum value below which thermo-mechanical reliability is significantly compromised.[7]

To improve the adhesion between such multifunctional coatings and polymer substrates, different strategies have been attempted that include changing the coating chemistry[8] and pretreating the surface of the polymer before coating deposition.[4] In those instances, incorporating carbon bridges in the inorganic silica network has

* Address correspondence to gdubois@us.ibm.com, dauskardt@stanford.edu.

Received for review April 18, 2014 and accepted July 2, 2014.

Published online July 02, 2014
10.1021/nn502161p

been shown to significantly increase adhesion to the polymer substrate.[8] Using plasma to modify the polymer surface to create more polar groups can significantly improve the adhesion with plasma-[4] and solution-based[6] oxide coatings, without compromising their bulk properties. In another example, adding a sol−gel-based siloxane soft layer between the polymer and a plasma-based SiO_xC_y hard coating dramatically improved the wear resistance of the coatings on the polymer.[9]

In this study, we demonstrate a general strategy to control the adhesive and the bulk properties of transparent protective coatings on polymers by depositing a bilayer structure using atmospheric plasma. The atmospheric plasma deposition process is particularly suitable for multilayer deposition because it provides easy and accurate control of the layer thickness, coating quality, and has a minimal waiting time between depositing different layers compared to solution-based deposition process (*e.g.*, the sol−gel process). At the same time, it is a low-cost, in-air, low-temperature, and large-scale process, especially suitable for depositing on large polymer substrates, compared to the conventional vacuum-based techniques (*e.g.*, CVD and sputtering in vacuum chambers).

This concept is demonstrated through the deposition of a highly adhesive and hard transparent bilayer coating on poly(methyl methacrylate) (PMMA) substrates. The bottom layer is adhesive organic−inorganic hybrid organosilicate, and the top layer is dense silica with high Young's modulus, hardness, and scratch resistance. In this system, a minimal thickness for the bottom adhesive layer is necessary to ensure maximum adhesion of the whole structure. The bilayer exhibits ~100% transmittance in the visible wavelength range, twice the adhesion energy of commercial polysiloxane sol−gel coatings and a 3-fold increase in Young's modulus.

RESULTS AND DISCUSSION

All the coatings in this work exhibited ~100% transmittance in the visible wavelength range (Figure 1). The single-layer coating adhesion and Young's moduli were found to exhibit a negative correlation for coatings deposited by atmospheric plasma using BTESE as the silica source precursor. Coatings with the highest Young's modulus had the lowest adhesion energy and *vice versa*. Alternatively, bilayer coatings were found to go against this trend with the possibility of both optimal adhesion and Young's modulus as we describe below.

Young's Modulus and Adhesion of Single Silica Layers. We chose three deposition conditions for coatings with either high Young's modulus or adhesion values and an intermediate condition as presented in Table 1. The effect of each deposition parameter on the coating properties will be published separately. The Young's

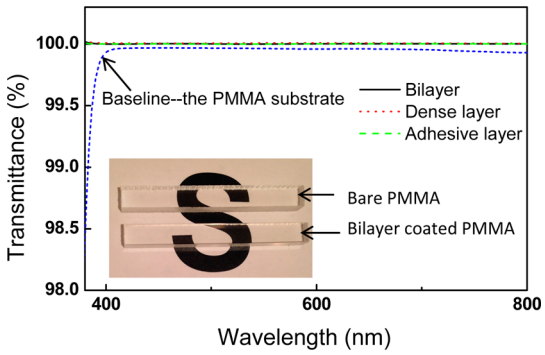

Figure 1. Visible transmittance of the bare PMMA substrate and the bilayer, dense, and adhesive coatings (baseline-corrected). The inset picture shows the visible transparency of a bilayer coating (adhesive layer 440 nm thick, and dense layer 120 nm thick) on PMMA.

TABLE 1. Deposition Conditions and Coating Properties of the Dense and Adhesive Layers

parameters	dense	intermediate	adhesive
plasma power (W)		60	
plasma gas (1% O_2 and 99% He) flow rate (L/min)	30	30	20
deposition distance (mm)	5	8	10
BTESE vapor pressure		1.6 Torr at 120 °C	
BTESE flow rate (L/min)	0.1	0.15	0.2
deposition rate (nm/min)	81	86	97

modulus and adhesion were affected by the coatings' molecular structure, especially by the ethyl bridge incorporation from the precursor (BTESE) molecule. As a result, the carbon content in the coatings can serve as a unique marker to optimize each individual layer. The Young's modulus or the adhesion of the single-layer organosilicate was optimized by tuning the plasma gas flow rate, the deposition distance, the BTESE flow rate, and the deposition rate.

The coating deposited at short deposition distance and low precursor flow rate (Table 1) exhibited the highest density of 1.730 g/cm^3 and Young's modulus of 18.9 GPa but the lowest adhesion energy to PMMA of 2.9 ± 0.9 J/m^2 (Figure 2 and Table 2). The high density and Young's modulus of this *dense* coating resulted from a highly connected Si−O−Si network at the molecular scale, as previously evidenced by IR.[8] Such a dense network usually contains low carbon remnants: 1.6 atom % of carbon was measured by XPS for this coating, as compared to 7.3 atom % for the low modulus coating. Young's modulus and hardness usually exhibit a strong positive correlation[10,11] and are both desirable to improve the polymer surface scratch resistance. However, the low adhesion of such coatings would limit their practical use.

When both the deposition distance and the BTESE flow rate were slightly increased (Table 1), a coating with lower Young's modulus and higher adhesion was

deposited (Figure 2 and Table 2). As the deposition distance and the BTESE flow rate were further increased with a lower plasma gas flow rate, a highly adhesive organosilicate coating was obtained. This *adhesive* coating had an adhesion to PMMA of 18.3 ± 2.1 J/m^2, a lower density of 1.675 g/cm^3, and a Young's modulus of 6.0 GPa (Figure 2 and Table 2). The significantly improved adhesion was related to the coating's higher carbon content (7.3 atom %) and the impact of the deposition conditions on the PMMA surface. When the precursor flow rate was high, more carbon bridges survived in the deposition process and then were incorporated into the coating, as evidenced by IR spectroscopy in previous work.[8]

The carbon bridge in the organosilicate network dramatically improves the coating's adhesion by a molecular bridging effect which increases energy dissipation when the coating is delaminated from the substrate.[12−14] Increasing the deposition distance and the precursor flow rate, and decreasing the plasma gas flow rate, also prevents overoxidation of the polymer substrate during coating deposition. This is critical for PMMA because we have shown previously that overexposure of PMMA to plasma prior to/during deposition promotes the formation of a low-molecular-weight layer which significantly disrupts the interaction between the coating and the bulk substrate and reduces adhesion.

It is worth noting that all the atmospheric plasma deposited BTESE coatings exhibited higher Young's modulus than typical commercial sol−gel polysiloxane coatings (~5 GPa).[3] Moreover, the adhesion energy of the most adhesive coating to PMMA was more than twice that of commercial sol−gel polysiloxane hard protective coatings (~8 J/m^2 in Figure 5 of ref 3) (Figure 2).

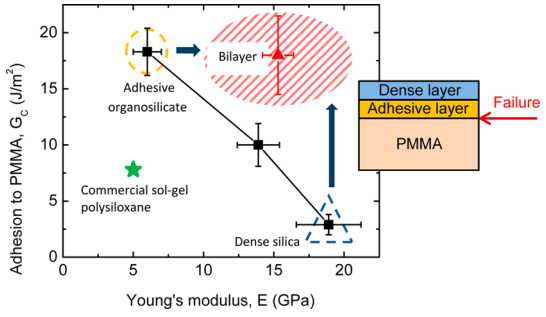

Figure 2. Relation between Young's modulus and adhesion energy to PMMA for the single layers and bilayers deposited using atmospheric plasma, and the commercial sol−gel polysiloxane coatings (Figure 5 of ref 3).

Bilayer Deposition To Couple High Young's Modulus with High Adhesion. The next step was to sequentially deposit two individual adhesive and dense layers on PMMA and demonstrate that both the high Young's modulus and the superior interfacial adhesion can be maintained in such a bilayer structure. We used the deposition conditions reported above (Table 1) to fabricate the dense and adhesive sublayers in the bilayer structure. The interface between the adhesive and dense layers should be strong because of the similarities between the two coatings and the plasma activation of the adhesive bottom layer during dense silica deposition. We anticipate that from a coating fracture point of view the bilayer coating would behave as a single layer as we demonstrate below (Figure 2). On the other hand, the chemical composition and density of the two sublayers sufficiently differ to be characterized by both XPS elemental depth profiling (Figure 3a) and X-ray reflectivity (Figure 3b).

The XPS elemental depth profiling provided the first direct evidence of the bilayer structure (Figure 3a). Since the adhesive and dense layers have different carbon contents (Table 2), the carbon percentage through the coating thickness was a good indication of the layer structure. At the surface, the carbon content was high because of hydrocarbon contaminants from the air. After 0.5 min of sputtering, the carbon content dropped to ~1.4 atom %, consistent with ~1.6 atom % for the dense silica single layer. At ~3 min sputtering, corresponding to ~54 nm coating depth, the carbon content began to increase at the dense/adhesive layer interface. Then at ~4 min sputtering, it stabilized at ~7 atom % in the adhesive organosilicate layer (~7.3 atom % carbon for the single adhesive layer). Finally, after 12.5 min sputtering, corresponding to ~380 nm total coating depth, the silicon and oxygen contents dropped and the carbon content increased, indicating that the PMMA substrate had been reached.

The XRR measurement also confirmed the bilayer structure (Figure 3b and Table 2). The through-thickness density profile of the coating can be deduced from the

TABLE 2. Properties of the Atmospheric Plasma Deposited Single Layers, Bilayer, and the Commercial Sol−Gel Polysiloxane Coatings

coating type	carbon content (atom %)	density (g/cm^3)	Young's modulus, *E* (GPa)	adhesion energy to PMMA, G_c (J/m^2)
dense	1.6	1.730	18.9	2.9 ± 0.9
intermediate	2.2	1.704	13.9	10.1 ± 1.3
adhesive	7.3	1.675	6.0	18.3 ± 2.1
bilayer	top: 1.4 bottom: ~7	top: 1.736 bottom: 1.660	average through thickness: 15.3	18.0 ± 3.5
commercial sol−gel polysiloxane			~5	~8

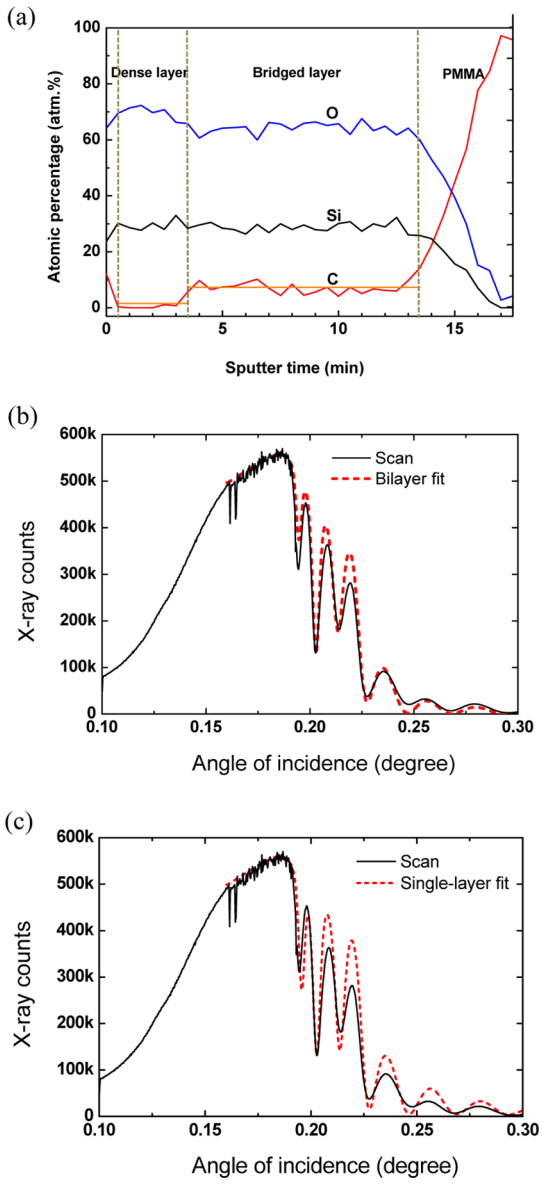

Figure 3. (a) XPS depth profile of the bilayer. The orange lines indicate the carbon percentage in the dense silica and adhesive organosilicate single layers measured by XPS, which are consistent with the bilayer depth profile. XRR scan and the curve fits of the bilayer, using (b) the bilayer model and (c) the single-layer model, also suggest the bilayer structure.

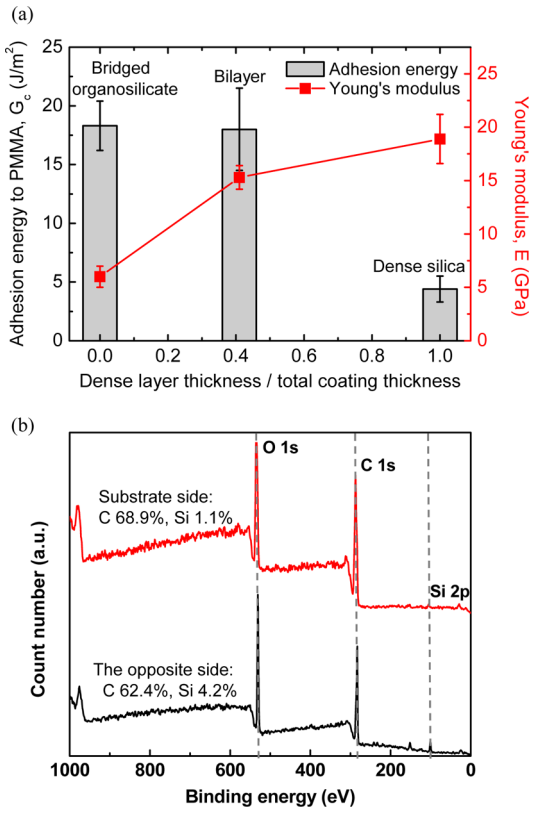

Figure 4. (a) Young's modulus and adhesion energy of the adhesive organosilicate, dense silica, and bilayer coatings on PMMA, with the *x*-axis as the dense layer *versus* total coating thickness. (b) Elemental XPS analysis of the fracture surface of the bilayer, showing delamination at the PMMA/adhesive organosilicate interface.

relative height, shape, and spacing of the interference fringes in the XRR graph. The best fits of the experimental data using a single-layer and a bilayer model are shown in Figure 3b,c. The bilayer model provided much better fit than the single-layer model. Moreover, the bilayer model provided an accurate density fit with top and bottom layer densities of 1.736 and 1.660 g/cm^3, respectively, in good agreement with the density measurements of the dense (1.754 g/cm^3) and adhesive (1.675 g/cm^3) single layers.

With the bilayer structure confirmed, we characterized its unique mechanical properties. The bilayer coating showed a high adhesion (18.0 $\pm$ 3.5 J/m^2) similar to the adhesive silica (Figures 2 and 4a). This adhesion value was for the bilayer/PMMA interface, as evidenced by the elemental composition of the fractured surfaces after the ADCB test. On the substrate side of the fractured surface, only a small remnant of silicon of ~1.1 atom % was detected, while on the coating side, there was slightly higher silicon content of ~4.2 atom % and a substantial amount of carbon species (Figure 4b). This result suggests that fracture occurred at the PMMA/adhesive layer interface, closer to the PMMA side, and that the interfacial adhesion of adhesive silica/dense silica was high enough to behave as an integrated coating during fracture. Interestingly, the adhesion of the bilayer to PMMA was not affected by top layer deposition or adhesion tests of up to 3 months after depositing the adhesive organosilicate layer. This provides additional flexibility in the deposition schedule for real applications.

At the same time, the Young's modulus of the bilayer (15.3 GPa) was greatly improved, compared to the adhesive silica single layer (6.0 GPa) (Figures 2 and 4a). These measurements were performed by SAWs which can only measure the Young's modulus of the bilayer as a whole, with the average density of the bilayer as an input. As a result, the actual Young's modulus and hardness of the top layer were underestimated.

The bilayers studied therefore exhibited significantly improved Young's modulus and adhesion to PMMA compared to single layers. An important question for the bilayer design is the ideal thickness requirement for each layer. We would anticipate that the Young's modulus and hardness of the dense layer are intrinsic material properties independent of thickness, while the adhesion of the adhesive layer may increase with thickness until reaching a plateau because more plastic energy would be consumed to delaminate a thicker adhesive coating. The critical adhesive layer thickness before reaching the adhesion plateau is an important bilayer parameter for applications.

Minimal Effective Thickness of the Adhesive Organosilicate Layer. As mentioned in the previous section, the carbon bridges in the coating contribute to a molecular bridging so that energy-consuming molecular relaxation occurs in a plastic deformation zone near the crack tip during coating delamination.[1,15,16] The plastic zone size in a thick coating is determined by the intrinsic coating properties (*i.e.*, yield stress, Young's modulus, and ductility of the coating). However, in a thin coating, the plastic zone size will be constrained by the coating thickness which limits the amount of plastic energy dissipated in the zone. As a result, the adhesion decreases with decreasing coating thickness below a critical coating thickness.[1,15,17,18]

The critical adhesive layer thickness was determined by varying the thickness of the adhesive layer from 50 to 430 nm while keeping the top dense layer at a constant thickness of 120 nm (Figure 5). A critical thickness of ~100 nm was observed for the adhesive layer, below which the adhesion of the bilayer decreased from a plateau of ~18 to 16.4 ± 2.1 J/m^2 at 80 nm layer thickness and 13 ± 2.4 J/m^2 at 50 nm layer thickness. We demonstrated a similar critical thickness value of ~100 nm for a plastic a-SiC:H thin film in a film structure containing a weak SiCN/nanoporous glass interface.[1] This present result verifies the plasticity contribution of the adhesive organosilicate layer and provides a minimum thickness guideline for the adhesive layer in a bilayer application.

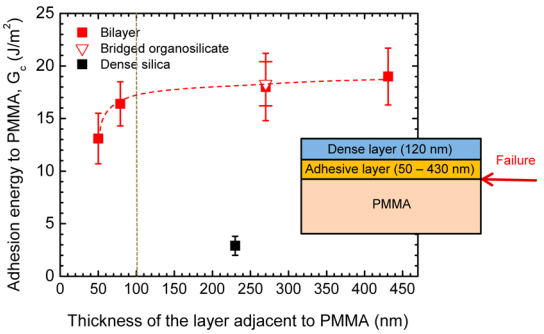

Figure 5. Minimal thickness threshold of the adhesive organosilicate layer to be fully effective.

CONCLUSION

We demonstrated hard, adhesive, and highly transparent bilayer protective coating deposition on PMMA in a single precursor, one-step deposition process, using atmospheric plasma. The bottom adhesive layer doubled the adhesion energy, and the top hard layer significantly improved the Young's modulus. The bilayer structure exhibited dramatically increased adhesion and Young's modulus at the same time and behaved as an integrated coating during fracture. The critical adhesive layer thickness was determined to be ~100 nm, which provides an important guideline for bilayer structure design. The single-layer and bilayer coatings exhibited ~100% transmittance in the visible wavelength range.

EXPERIMENTAL METHOD

Coating Deposition. Coatings were deposited using an atmospheric pressure plasma system (Surfx Technologies LLC, Redondo Beach, CA) integrated with a high-temperature precursor delivery system.[8] The 99.995% purity helium and oxygen (Praxair Inc., Santa Clara, CA) were mixed and fed into the capacitive discharge plasma. The plasma was driven by 13.56 MHz radio frequency power. The adhesive and dense silica layers as well as a reference coating were deposited using the same carbon-bridged organosilane precursor, 1,2-bis(triethoxysilyl)ethane (BTESE) (Gelest, Inc. Morrisville, PA) under different plasma and precursor delivery conditions (Table 1). The detailed deposition method was reported previously.[8]

Coatings were deposited on military grade stretched PMMA sheets meeting all requirements of MIL-PRF-25690 and on silicon wafers. The substrate was wiped with ethanol before deposition to remove any surface contamination and dust and then dried in air for 24 h. Deposition of a uniform coating with controlled thickness was implemented through the use of an *X*−*Y*−*Z* stage that moved the plasma source over the substrate in a planar fashion, forming a rectangular array. The coating thickness can be controlled by the scanning speed of the plasma source and the number of passes during deposition. When a bilayer was deposited, the top layer was deposited with 0−3 months waiting time after the deposition of the bottom layer.

Characterization Methods. The coating thickness was characterized by ellipsometry (Woollam M2000, J. A. Woollam Inc., Lincoln, NE). Incident light (45° polarization) at the Brewster angle of the substrate was used to maximize reflection. The polarization *versus* wavelength of the reflected light was first measured for the coating on the silicon substrate. The silicon substrate properties were used to fit the refractive index and absorbance of the coating by regressive analysis. Then a spectrum was taken for the bare PMMA substrate (wavelengths between 250 and 1000 nm). Finally, a spectrum was taken for the coating on the PMMA substrate. The thickness of either the single layer or the bilayer was fitted based on the measured refractive index and absorbance of the coatings and the spectrum of the PMMA substrate.

The visible transmittance of the coatings (thickness ~500 nm) was measured by a UV−vis−NIR spectrophotometer (Cary 6000i, Agilent Technologies Inc., USA). The average transmittance was calculated by averaging the values obtained for the wavelength in the range of 380 to 800 nm.

The density, ρ, of the coating on the silicon substrate was measured by specular X-ray reflectivity (XRR) using a diffractometer (X'Pert Pro MRD, Panalytical, Westborough, MA) with

ceramic X-ray tube (wavelength = 0.154 nm) and high-resolution horizontal goniometer (reproducibility ±0.0001°). The coatings' density and thickness were determined through data fitting of the X-ray counts *versus* incidence angle, using the genetic algorithm of X'Pert Reflectivity software. The number of layers set in each fit matched the number of layers experimentally deposited. The layers were modeled as organosilicate materials with the following average composition CH_3SiO_2.

The Young's modulus was obtained using surface acoustic wave spectroscopy (SAWS). SAWS studies were performed with a laser-acoustic thin film analyzer (LaWave, Fraunhofer USA, Boston, MA) in which acoustic waves were generated by a nitrogen pulse laser (wavelength 337 nm, pulse duration 0.5 ns). These were detected using a transducer employing a piezoelectric polymer film sensor. The measured surface wave velocity as a function of frequency was fitted with the theoretical dispersion curve to deduce Young's modulus (a value of 0.25 was assigned for Poisson's ratio).

The adhesion energy of the coating on PMMA was quantified using the asymmetric double cantilever beam (ADCB) test.[3,19−21] The specimens were prepared by gluing an uncoated thinner substrate onto a coated thicker substrate. The in-plane dimensions of the specimen were 9 mm × 70 mm. The thicknesses of the uncoated and coated substrates were 3 and 6 mm, respectively. The fracture tests were conducted on a micromechanical adhesion test system (DTS Delaminator Test System, DTS Company, Menlo Park, CA) in displacement control mode. The specimens were loaded (displacement rate = 5 μm/s) in tension to produce controlled crack growth, followed by unloading. The load was measured simultaneously, and the adhesion energy, G_c (J/m^2), was calculated from the critical value of the strain energy release rate.[3,19−21] Application of the technique to thin hard coatings on softer substrates similar to the types in the present study has been previously reported.[3,8]

The elemental composition of the coatings and the fracture surfaces after adhesion test was analyzed by X-ray photoelectron spectroscopy (XPS) (Physical Electronics Inc., Chanhassen, MN). An Al Kα (1486 eV) X-ray source was used (spot size ∼1 mm, pass energy 117.4 eV, scan range 0 to 1000 eV). Before the coating composition was measured, surface contamination was removed by argon ion beam sputtering (sputter time ∼4 min). An elemental depth profile of the bilayer was also probed with alternate argon ion beam sputtering (1 kV, 0.5 μA, beam size 2 mm × 2 mm, sputter rate ∼18 nm/min for the dense silica and ∼35 nm/min for the adhesive organosilicate coating, and 0.5 min acquisition time interval).

Conflict of Interest: The authors declare no competing financial interest.

Acknowledgment. The work was supported in part by the Director, Office of Energy Research, Office of Basic Energy Sciences, Materials Sciences Division of the U.S. Department of Energy, under Contract No. DE-FG02-07ER46391, and by Boeing Company.

REFERENCES AND NOTES

1. Matsuda, Y.; Ryu, I.; King, S. W.; Bielefeld, J.; Dauskardt, R. H. Toughening Thin-Film Structures with Ceramic-like Amorphous Silicon Carbide Films. *Small* **2014**, *10*, 253–257.
2. Dupont, S. R.; Oliver, M.; Krebs, F. C.; Dauskardt, R. H. Interlayer Adhesion in Roll-to-Roll Processed Flexible Inverted Polymer Solar Cells. *Sol. Energy Mater. Sol. Cells* **2012**, *97*, 171–175.
3. Kamer, A.; Larson-Smith, K.; Pingree, L. S. C.; Dauskardt, R. H. Adhesion and Degradation of Hard Coatings on Poly(methyl methacrylate) Substrates. *Thin Solid Films* **2011**, *519*, 1907–1913.
4. Cui, L.; Ranade, A. N.; Matos, M. A.; Dubois, G.; Dauskardt, R. H. Improved Adhesion of Dense Silica Coatings on Polymers by Atmospheric Plasma Pretreatment. *ACS Appl. Mater. Interfaces* **2013**, *5*, 8495–8504.
5. Shenton, M. J.; Lovell-Hoare, M. C.; Stevens, G. C. Adhesion Enhancement of Polymer Surfaces by Atmospheric Plasma Treatment. *J. Phys. D: Appl. Phys.* **2001**, *34*, 2754–2760.
6. Lionti, K.; Cui, L.; Volksen, W.; Dauskardt, R.; Dubois, G.; Toury, B. Independent Control of Adhesive and Bulk Properties of Hybrid Silica Coatings on Polycarbonate. *ACS Appl. Mater. Interfaces* **2013**, *5*, 11276–11280.
7. Brand, V.; Bruner, C.; Dauskardt, R. H. Cohesion and Device Reliability in Organic Bulk Heterojunction Photovoltaic Cells. *Sol. Energy Mater. Sol. Cells* **2012**, *99*, 182–189.
8. Cui, L.; Ranade, A. N.; Matos, M. A.; Pingree, L. S.; Frot, T. J.; Dubois, G.; Dauskardt, R. H. Atmospheric Plasma Deposited Dense Silica Coatings on Plastics. *ACS Appl. Mater. Interfaces* **2012**, *4*, 6587–6598.
9. Coak, C. E.; Sundaram, V. S.; Wascher, W. W. Durable Transparent Coatings for Aircraft Passenger Windows. US Patent 8313812 B2 2012.
10. Beake, B. D.; Smith, J. F. High-Temperature Nanoindentation Testing of Fused Silica and Other Materials. *Philos. Mag. A* **2002**, *82*, 2179–2186.
11. Liou, H.-C.; Pretzer, J. Effect of Curing Temperature on the Mechanical Properties of Hydrogen Silsesquioxane Thin Films. *Thin Solid Films* **1998**, *335*, 186–191.
12. Dubois, G.; Volksen, W.; Magbitang, T.; Miller, R. D.; Gage, D. M.; Dauskardt, R. H. Molecular Network Reinforcement of Sol−Gel Glasses. *Adv. Mater.* **2007**, *19*, 3989–3994.
13. Maidenberg, D. A.; Volksen, W.; Miller, R. D.; Dauskardt, R. H. Toughening of Nanoporous Glasses Using Porogen Residuals. *Nat. Mater.* **2004**, *3*, 464–469.
14. Matsuda, Y.; Kim, N.; King, S. W.; Bielefeld, J.; Stebbins, J. F.; Dauskardt, R. H. Tunable Plasticity in Amorphous Silicon Carbide Films. *ACS Appl. Mater. Interfaces* **2013**, *5*, 7950–7955.
15. Litteken, C.; Dauskardt, R. Adhesion of Polymer Thin-Films and Patterned Lines. *Int. J. Fract.* **2003**, *120*, 475–485.
16. Rowland, H. D.; King, W. P.; Pethica, J. B.; Cross, G. L. W. Molecular Confinement Accelerates Deformation of Entangled Polymers during Squeeze Flow. *Science* **2008**, *322*, 720–724.
17. Dauskardt, R. H.; Lane, M.; Ma, Q.; Krishna, N. Adhesion and Debonding of Multi-layer Thin Film Structures. *Eng. Fract. Mech.* **1998**, *61*, 141–162.
18. Volinsky, A. A.; Moody, N. R.; Gerberich, W. W. Interfacial Toughness Measurements for Thin Films on Substrates. *Acta Mater.* **2002**, *50*, 441–466.
19. Kanninen, M. F. Augmented Double Cantilever Beam Model for Studying Crack-Propagation and Arrest. *Int. J. Fract.* **1973**, *9*, 83–92.
20. Suo, Z. G.; Hutchinson, J. W. Sandwich Test Specimens for Measuring Interface Crack Toughness. *Mater. Sci. Eng., A* **1989**, *107*, 135–143.
21. Anderson, T. L. *Fracture Mechanics: Fundamentals and Applications*; CRC Press: Boca Raton, FL, 2005.